DFT Study of Conformational and Spectroscopic Properties of Yatakemycin

Fabio Pichierri*

COE Laboratory, Tohoku University, IMRAM, 2-1-1 Katahira, Sendai 980-8577, Japan

Vinicio Galasso

Dipartimento di Scienze Chimiche, Universitá di Trieste, I-34127 Trieste, Italy

Received: March 7, 2007; In Final Form: April 30, 2007

Molecular structure and conformational preferences of yatakemycin, a novel and exceptionally potent antitumor agent, have been investigated using the density functional theory (DFT) formalism. From the relative stability of various possible conformations, it is found that two conformers are nearly isoenergetic and markedly more stable than the others in the gas phase. To test the effect of polar mediums, the relative energies have been recalculated using the self-consistent reaction field method. Thus, the most stable conformer of the isolated molecule in the gas phase is expected to be still more preferred in solution. The molecular structure of yatakemycin has also been studied by means of its spectroscopic properties. The DFT results satisfactorily reproduce the experimental data and corroborate the reliability of the structural characterization advanced for yatakemycin. The lowest-energy electronic transitions have been interpreted with time-dependent DFT calculations. Notably, the strong IR band observed at 2852 cm^{-1} is unambiguously assigned to the O−H stretching of the $(C_7)O-H\cdots O(C_{12})$ fragment, linked by a strong intramolecular H-bond, and may be viewed as a distinctive fingerprint of yatakemycin. Furthermore, the calculated set of NMR chemical shifts of carbonyl carbon atoms and indole protons, the most sensitive to stereoelectronic factors, is consistent with experiment. The effects of both protonation and oxidation on the geometry of the most stable conformer have also been studied. With reference to yatakemycin's DNA alkylation properties, the structure of the yatakemycin−adenine adduct has been theoretically modeled and found to be consistent with experimental spectroscopic evidence.

1. Introduction

Yatakemycin (YM) is an antifungal antibiotic recently isolated by Igarashi and co-workers from the culture broth of *Streptomyces* sp. TP-AO356.[1] Like duocarmycin A, duocarmycin SA, and CC-1065, YM also possesses the ability to alkylate the DNA bases thereby exerting its cytotoxicity against cancer cells.[2] The original structural assignment, which was based on a combination of mass spectrometry and 2D NMR, IR, and UV−visible spectroscopic measurements, provided the chemical structure shown on the top part of Figure 1. Here, the YM molecule appears to be made of a central cyclopropapyrroloindole moiety (i.e., the DNA alkylation unit) bridging a sulfur-containing pyrroloindole moiety (left-hand) and an indole moiety (right-hand), each connected through an amide linkage. Subsequent synthetic studies carried out independently by the groups of Boger and Fukuyama[3−5] and triggered by its potential application as an anticancer drug, showed that (i) the methoxy and hydroxy groups on the indole moiety should be interchanged in position and (ii) the pyrroloindole moiety bears a thiomethyl ester subunit versus a thioacetate group, as shown on the bottom part of Figure 1.

A cursory look at Figure 1 suggests a nearly planar molecular structure for YM. However, the lack of an experimental crystal structure determination maintains a veil on the possibility that some distortion from planarity may occur in the molecule.

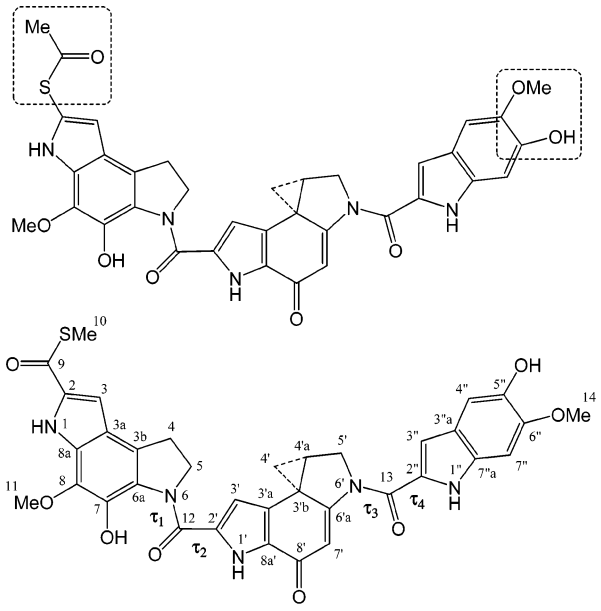

Figure 1. Original (top) and revised (bottom) formula of YM together with atom numbering and the four torsion angles determining the conformational preferences.

Furthermore, the presence of various torsion angles in the molecule suggests that YM might exist as a mixture of some conformers.

Because a detailed knowledge of the structure and spectroscopic properties of YM is an essential prerequisite for

* Corresponding author. E-mail: fabio@che.tohoku.ac.jp. Present address: Department of Applied Chemistry, Graduate School of Engineering, Tohoku University.

10.1021/jp071851x CCC: $37.00
Published on Web 06/12/2007

understanding its potent biological activity, an accurate theoretical investigation on YM seemed timely. In the present study, we used modern density functional theory (DFT) methods to explore the geometries and relative energies of the most stable conformers of YM, its electronic transitions, vibrational frequencies, NMR chemical shifts, and optical activity. The effects of both protonation of backbone nitrogen atoms and oxidization of the thiomethyl group on the geometry of the most stable conformer of YM were also investigated. Furthermore, we report on the results of DFT modeling of the YM−adenine adduct that mimics the site of nucleophilic attack and the structure of the DNA alkylation product.

2. Computational Details

All the quantum-chemical calculations were performed with the Gaussian 03 software package.[6] Geometry optimizations and frequency calculations were carried out using the BLYP method[7,8] in combination with the 6-31G(d, p) basis set. By employing this pure exchange-correlation functional, full advantage has been taken from the automatic density fitting method of Dunlap.[9] Harmonic frequency calculations were performed for all the optimized structures to establish that the stationary points are minima. The vibrational characterization was based on the normal-mode analysis performed according to the Wilson FG matrix method,[10] using standard internal coordinates and the scaling factors of Rauhut and Pulay.[11] Localization of the molecular orbitals (MOs) was performed by means of the Pipek−Mezey procedure,[12] and bond order indices were calculated from the definition of Sannigrahi and Kar.[13]

The specific optical rotation at the sodium D line $[\alpha]_D$ was calculated with the time-dependent (TD) DFT method[14] using the B3LYP hybrid functional of Becke.[15] The cc-pVDZ valence basis set[16] was augmented with 2s2p2d uncontracted diffuse functions (s exponents, 0.0624 and 0.2758; p exponents, 0.0550 and 0.2574; d exponents, 0.2377 and 0.2787) placed at the center of mass of the molecule. Gauge-invariant atomic orbitals (GIAOs) were used to provide origin-independent results.

Vertical excitation energies and oscillator strengths were calculated with the TD-DFT method,[17] employing the B3LYP functional and the cc-pVDZ basis set.

The ^{1}H and ^{13}C NMR absolute shielding constants (σ values) were computed using the continuous set of gauge transformations (CSGT) method[18] using the 6-311G(2d, p) basis set. The calculated magnetic shieldings were converted into the δ chemical shifts by noting that at the same level of theory the ^{1}H and ^{13}C absolute shieldings in tetramethylsilane (TMS) are 31.23 and 175.44, respectively.

3. Results and Discussion

3.1. Conformational Properties. YM has four main rotation axes (two C−C and two C−N bonds) that give rise to conformational isomers. The relevant torsion angles can be specified as τ_1(O−C_{12}−N_6−C_{6a}), τ_2(O−C_{12}−$C_{2'}$−$C_{3'}$), τ_3(O−C_{13}−$N_{6'}$−$C_{6'a}$), and τ_4(O−C_{13}−$C_{2''}$−$C_{3''}$), as shown in Figure 1. Schematically, the central part of the molecule is kept frozen and each lateral unit is allowed to turn upon it in two different ways.

On the basis of a careful analysis of the potential energy map of YM and preliminary empirical calculations, the number of the most favorable structures to be considered for full optimization is 12. Common to all DFT-optimized conformers is that their molecular shape resembles an approximately planar sheet, except for the central cyclopropane ring that is nearly orthogonal to the conjugated cyclohexadienone π-system. In particular, the two most preferred conformers YM1 ($\tau_1 = -2.6°$, $\tau_2 = 165.9°$, $\tau_3 = 8.0°$, $\tau_4 = -170.7°$) and YM2 ($\tau_1 = -2.7°$, $\tau_2 = 165.3°$, $\tau_3 = -150.9°$, $\tau_4 = -162.8°$) correspond to the structures depicted in Figure 2. In these conformers, the distance connecting the C_{10} atom of the thiomethyl group to the C_{14} atom of the methoxy group is 26.1 Å (YM1) and 26.2 Å (YM2). Tables containing the Cartesian coordinates of these two conformers are given in the Supporting Information.

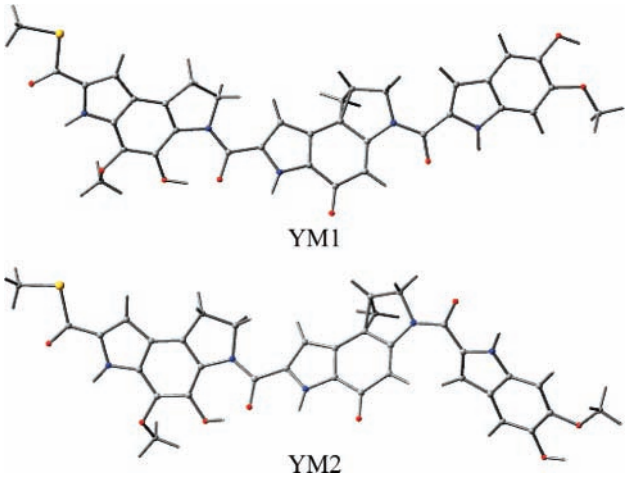

Figure 2. DFT-optimized geometries of YM1 (top) and YM2 (bottom).

A noteworthy point is that, in the gas phase, the lowest-energy conformer YM1 is preferred by only 0.13 kcal mol^{-1} over conformer YM2 but is at least 2.45 kcal mol^{-1} more stable than the other conformers. On the other hand, it is interesting to note that, according to our DFT results, the conformer YM1, incorporating the thiomethyl ester, is 7.16 kcal mol^{-1} lower in energy than the most stable conformer of the "original" structure (Figure 1) bearing the thioacetate group. Of course, energetic stability should not be the sole criterium that one has to adopt for the correct structural assignment of a natural product. Indeed, alternative low-energy structures may be readily tested with state-of-the-art theoretical methods. In this regard, a reliable verification of a new molecular structure relies on calculation of spectroscopic properties that can be compared with experiment. As an interesting example of a computer-aided investigation of natural products, we mention the structure revision of hexacyclinol recently reported by Rychnovsky.[19]

Because the biological activity of YM occurs in solution, it was considered important to gain some information on its conformational preferences in a solvated environment. Thus, for each conformer, the gas-phase equilibrium structure was completely re-optimized at the DFT level with the polarization continuum model (PCM)[20] in water solution (dielectric constant $\epsilon = 78.39$). The DFT values of the torsion angles and the energy relative to the most stable conformer are given in Table 1. These results indicate a stronger preference for conformer YM1 in water solution than in the gas-phase. On this basis, one may speculate that a mixture of the two most preferred conformers YM1 and YM2 exists in the gas phase (about 50:50%) and in water solution (72:28%), assuming thermal equilibrium at 25 °C. A similar situation is also predicted (with single-point PCM calculations) in dimethylformamide solution (DMF, $\epsilon = 36.71$, solvent radius = 2.647 Å;[21] 77:23%) and in methanol solution ($\epsilon = 32.63$; 81:19%).

One particularly interesting point is that, for all conformers studied, the DFT calculations gave an intramolecular H-bond between two neighboring hydroxy and carbonyl groups. In YM1

TABLE 1: Torsion Angles (Deg), Relative Energies (kcal mol^{-1}), and Dipole Moments (Debye) of YM Conformers in Water Solution

conformer	τ_1	τ_2	τ_3	τ_4	ΔE^a	μ
YM1	−2.5	160.9	8.9	−165.8	0	15.2
YM2	−2.4	161.1	−147.7	−157.4	0.58	12.6
YM3	−2.3	−31.2	8.7	−166.3	2.35	10.7
YM4	−1.8	160.9	12.4	27.6	2.36	18.6
YM5	−1.9	−30.9	−48.5	−157.6	3.07	9.7
YM6	−4.7	165.9	−145.7	10.1	3.11	7.3
YM7	−2.6	162.4	140.9	152.1	5.29	11.0
YM8	−3.2	−21.4	−144.3	12.1	6.48	7.3
YM9	−1.3	−33.0	−145.8	21.6	12.22	9.1
YM10	−2.8	160.9	138.8	149.5	12.30	13.5
YM11	−3.2	164.9	132.0	−18.3	14.31	10.3
YM12	−2.5	−30.2	138.5	149.3	14.87	11.0

[a] Inclusive of zero-point energy contribution.

(gas-phase), the relevant parameters in the slightly bent (C_7)O−H···O(C_{12}) unit are O−H 1.019 Å, H···O 1.540 Å, O···O 2.539 Å, and angle O−H···O 165.5°. The strong engagement of the carbonyl oxygen atom in this H-bond is also reflected in the sizable lengthening of the C_{12}═O bond (1.271 Å), compared with the other "normal" C═O bonds: C_9═O (1.237 Å), $C_{8'}$═O (1.248 Å), and C_{13}═O (1.249 Å). Further discussion on this point is postponed till the analysis of vibrational frequencies.

Another notable aspect concerns the central cyclopropane ring that is strongly involved in the bioactivity of YM. For YM1 (gas-phase), the DFT-computed bond lengths are 1.540 Å ($C_{3'b}$−$C_{4'a}$), 1.557 Å ($C_{3'b}$−$C_{4'}$), and 1.503 Å ($C_{4'a}$−$C_{4'}$) that are in line (albeit relatively longer) with the X-ray values determined for related N-aryl derivatives of 1,2,9,9a-tetrahydrocyclopropa-[*c*]benz[*e*]indol-4-one (CBI).[22] The relevant bond order index is 0.925 for $C_{3'b}$−$C_{4'a}$, 0.874 for $C_{3'b}$−$C_{4'}$, and 0.910 for $C_{4'a}$−$C_{4'}$. This calculated structural pattern is therefore consistent with exclusive $C_{4'}$ nucleophilic addition with cleavage of only the weaker (longer) $C_{3'b}$−$C_{4'}$ cyclopropane bond, as established with the formation of the YM−adenine adduct.[5]

A clue on reactivity of YM is also provided by the electric dipole moment. The DFT values (in water solution), reported in Table 1, reflect significant differences in the overall distribution of charge in the various conformers. Notably, among the lower energy conformers, the most stable conformer YM1 possesses a large dipole moment (15.2 Debye). In YM1, the dipole moment vector is approximately oriented along the central direction that joins $C_{3'}$ to H($C_{4'a}$).

As a final comment on the structure, it must be stressed that the absolute configuration of the natural product has been established as (+)-YM on the basis of the strong dextrorotatory $[\alpha]_D$.[1] The DFT calculated specific optical rotation $[\alpha]_D$ in vacuum is +109.7 for YM1 and −109.1 for YM2. However, for an equilibrium mixture of these conformers with the ratio 77:23% (as suggested by our PCM calculations), the DFT total specific rotation is +59.4, with sign and magnitude consistent with the experimental value of +100 in DMF solution.[1]

3.2. Spectroscopic Properties. Among the various spectroscopic observables, the electronic transitions, the vibrational frequencies, and NMR chemical shifts are very efficient monitors of the complex interplay of structural and electronic effects operating in a molecule. Therefore, we report on these properties in the following sections.

3.2.1. Electronic Transitions. The UV−visible absorption spectrum of YM in methanol solution (Figure 3) exhibits two strong bands peaked at 388 and 210 nm, separated by a complex envelope with four moderately intense shoulders discernible around 350, 310, 278, and 240 nm.[1] From an empirical

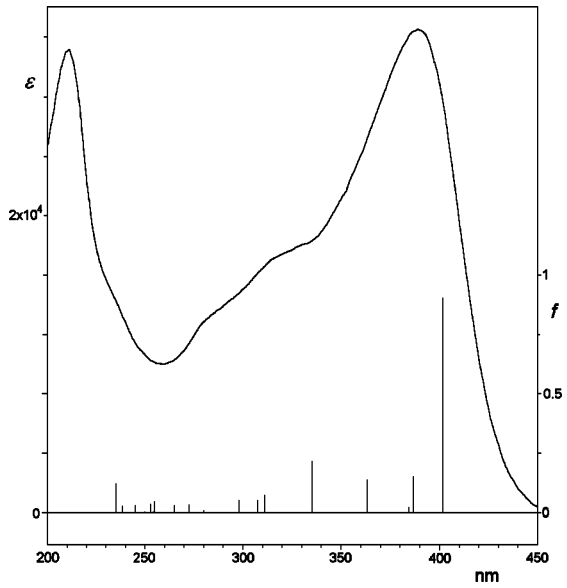

Figure 3. Electronic absorption spectrum of YM measured in methanol (λ in nm and ϵ in L mol^{-1} cm^{-1}; from ref 1) and electronic transitions calculated for YM1, displayed in the spike form.

standpoint, our fit to a sum of six Gaussian functions reproduced the entire absorption curve accurately.

The YM molecule, formed by three polycyclic conjugated moieties connected by amide linkages, has many interacting chromophoric groups that generate a crowd of closely spaced excited states. From a qualitative standpoint, the main electronic excitations of YM should bear a $n \rightarrow \pi^*$ and/or $\pi \rightarrow \pi^*$ character. However, as a result of a complex balance of conjugative and inductive effects and through-bond and through-space interactions, the various *n*(N, O, S) semilocalized orbitals are significantly mixed and the π orbitals are not restricted within a single polycyclic moiety but spread over the entire molecular skeleton. Furthermore, the nonplanarity of the molecule relaxes the separation of the σ and π frameworks. As illustrative examples, the first five (occupied and vacant) frontier MOs of the preferred conformer YM1 are shown in Figures 4 and 5. All of these MOs are of essential π character. However, there are important topological differences. In the HOMO, the π network is delocalized only over the left-hand pyrroloindole moiety. Upon descending along the top occupied MOs, the π network shifts progressively from the left to the right-hand unit, as shown in Figure 4. Thus, it mainly involves the lateral indole moiety in HOMO-3 whereas the central pyrroloindole moiety in HOMO-4. In the LUMO, the π network instead is concentrated over the central moiety but also propagates into the right-hand indole unit through the amidic relay. When proceeding along the LUMO series, the π network covers the right-hand unit, as shown in Figure 5. In LUMO+2, it encompasses the full molecular skeleton.

Given the complex electronic pattern of YM, it is very cumbersome to give a detailed analysis of the excitation processes responsible for the prominent features which appear in the absorption spectrum. Thus, only an essential overview of the salient aspects is presented here.

The TD-DFT results for YM1 are gathered in Table 2, together with the experimental results and are also displayed in Figure 3. In this respect, it is worthwhile to mention that previous reports place transition energies given by TD-DFT within approximately 0.3 eV of experimental values.[17,23,24] According to TD-DFT results, a number of transitions contribute to each of the bands observed in the absorption spectrum of

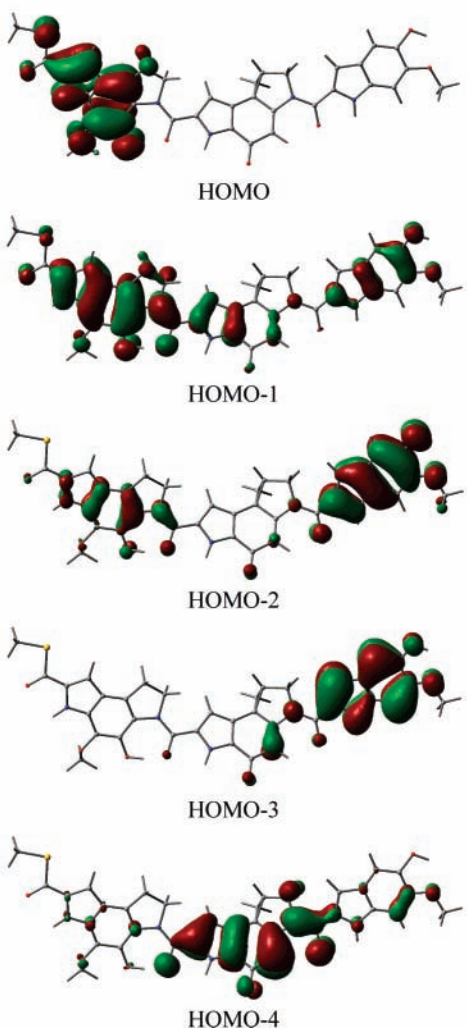

Figure 4. Frontier Kohn−Sham orbitals of YM1: HOMO, HOMO-1, HOMO-2, HOMO-3, and HOMO-4, from top to bottom.

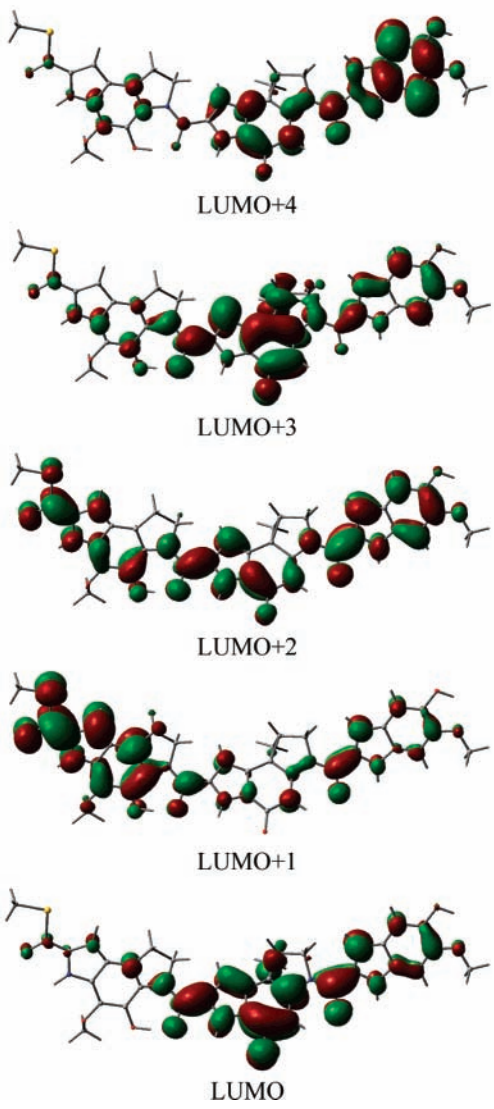

Figure 5. Frontier Kohn−Sham orbitals of YM1: LUMO, LUMO+1, LUMO+2, LUMO+3, and LUMO+4, from bottom to top.

YM. In particular, the lowest-energy band at 388 nm can be associated with the second predicted (strong, oscillator strength $f = 0.9010$) electronic transition, whose major component is the excitation HOMO-1 → LUMO ($\pi \rightarrow \pi^*$). This transition is flanked by other less intense transitions. Notably, the HOMO → LUMO ($\pi \rightarrow \pi^*$) excitation is the principal contributor to the lowest-energy (weakly allowed) electronic transition of YM, which is likely hidden under the prominent band centered at 388 nm. By reference to Figures 4 and 5, this process can be described as an intramolecular charge-transfer from the left-hand unit (the electron donor) to the right-hand unit (the electron acceptor).

The rather strong transition (mainly involving a π charge redistribution within the two lateral units), calculated at 345 nm and surrounded by two relatively intense satellites, should give rise to the distinct shoulder found around 350 nm in the absorption spectrum. On the other hand, each of the shoulders around 310, 278, and 240 nm can be attributed to a manifold of closely spaced ($\pi \rightarrow \pi^*$) transitions.

Unfortunately the TD-DFT formalism for a molecule as large as YM is computationally very heavy, thus only the lowest fifty excited states have been calculated. However, this output shows the generation of a congested multitude of transitions upon increasing energy. Therefore, no conclusive picture may be provided about the strong band observed at 210 nm, which is likely due to many transitions of mixed ($\pi \rightarrow \pi^*$) and ($n \rightarrow \pi^*$) nature.

3.2.2. Vibrational Frequencies. A selection of the most relevant DFT frequencies, with related potential energy distribution (PED in %) and assignment, are reported in Table 3 together with the IR experimental values.[1,4] First, it must be noted that the calculated vibrational pattern undergoes only minor changes on passing from YM1 to YM2. The most important vibrational feature of YM concerns the strong band observed at 2852 cm^{-1}, falling well apart from the prominent band system with onset at 2885 cm^{-1} and maximum at 2925 cm^{-1} that encompasses the manifold of closely lying C−H stretchings. Indeed, the present DFT results unambiguously assigned the band at 2852 cm^{-1} to the O_7−H stretching mode (for YM1: frequency 2826 cm^{-1}, intensity 48.7 D^2 $Å^{-2}$ amu^{-1}, and PED 99%). The large displacement of this mode to lower frequency (about 500−600 cm^{-1}) relative to the broad band of $O_{5''}$−H and N−H vibrations, with maxima at 3312 and 3450 cm^{-1},[1,4] is a clear manifestation of the strong intramolecular H-bond operative in the $(C_7)O-H\cdots O(C_{12})$ fragment. On the other hand, the higher frequency band at 2925 cm^{-1} belongs to stretchings of methyl and methylenic C−H bonds. Therefore, the strong band at 2852 cm^{-1} may be recognized as a distinctive fingerprint of YM.

TABLE 2: Electronic Transitions: Energies (eV and nm) and Intensities (Oscillator Strength *f*, Molar Absorptivity ϵ)

calcd E(eV)	λ (nm)	f	composition of wavefunction[a]	expt[b] λ (ϵ)
2.79	444.3	0.0087	0.68 (H → L) + 0.11 (H → L + 2)	
3.09	400.9	0.9010	0.66 (H − 1 → L) − 0.11 (H − 4 → L)	388 (32 600)
3.20	387.3	0.1513	0.58 (H → L + 1) − 0.23 (H − 2 → L)	
3.23	383.9	0.0218	0.62 (H − 2 → L) + 0.23 (H → L + 1)	
3.30	375.2	0.0012	0.62 (H − 6 → L) − 0.15 (H − 6 → L + 3)	
3.38	366.4	0.0311	0.53 (H → L + 2) − 0.27 (H − 1 → L + 2)	
3.41	363.4	0.1428	0.61 (H − 3 → L) − 0.16 (H − 1 → L + 1)	
3.59	345.1	0.5695	0.49 (H − 1 → L + 1) + 0.36 (H → L + 2)	350 (sh)
3.70	335.0	0.2111	0.46 (H − 2 → L + 1) − 0.32 (H − 4 → L)	
3.80	326.6	0.0146	0.59 (H − 1 → L + 2) − 0.19 (H − 2 → L + 2)	
3.82	324.8	0.0626	0.47 (H − 4 → L) + 0.35 (H − 2 → L + 1)	
3.90	317.6	0.0043	0.49 (H − 2 → L + 2) + 0.28 (H − 3 → L + 1)	
3.99	311.1	0.0709	0.56 (H → L + 3) + 0.31 (H − 3 → L + 1)	
4.00	310.0	0.0781	0.47 (H − 3 → L + 1) − 0.36 (H → L + 3)	310 (sh)
4.03	307.7	0.0518	0.56 (H − 5 → L) − 0.14 (H − 9 → L)	
4.15	298.6	0.0503	0.61 (H − 3 → L + 2) + 0.26 (H − 3 → L + 1)	
4.20	294.9	0.0009	0.57 (H − 10 → L + 1) + 0.27 (H − 10 → L + 2)	
4.22	293.6	0.0054	0.63 (H − 7 → L) − 0.23 (H − 7 → L + 1)	
4.27	290.6	0.0769	0.58 (H − 1 → L + 3) − 0.20 (H − 11 → L)	278 (sh)
4.29	289.3	0.0559	0.43 (H − 11 → L) + 0.25 (H − 1 → L + 3)	
4.35	284.9	0.0163	0.53 (H − 4 → L + 1) − 0.25 (H − 5 → L + 1)	
4.37	283.7	0.0014	0.45 (H − 5 → L + 1) − 0.35 (H − 2 → L + 3)	
4.39	282.3	0.0030	0.53 (H − 2 → L + 3) + 0.21 (H − 5 → L + 1)	
4.42	280.3	0.0197	0.54 (H − 7 → L + 1) + 0.22 (H − 7 → L)	
4.47	277.3	0.0010	0.43 (H − 9 → L) + 0.23 (H − 4 → L + 1)	
4.49	276.4	0.0077	0.40 (H − 6 → L + 1) − 0.30 (H − 11 → L)	
4.55	272.6	0.0347	0.54 (H − 4 → L + 2) + 0.26 (H − 3 → L + 3)	
4.60	269.8	0.0148	0.47 (H − 3 → L + 3) − 0.42 (H − 5 → L + 2)	
4.65	266.8	0.0470	0.35 (H − 3 → L + 3) + 0.31 (H − 5 → L + 2)	
4.68	264.9	0.0291	0.52 (H − 8 → L) − 0.24 (H − 9 → L)	
4.71	263.2	0.0020	0.51 (H − 6 → L + 2) + 0.39 (H − 6 → L + 1)	
4.73	262.2	0.0027	0.40 (H − 13 → L) − 0.28 (H − 8 → L)	
4.85	255.4	0.0128	0.59 (H − 7 → L + 2) − 0.21 (H − 7 → L + 1)	
4.87	254.6	0.0437	0.36 (H → L + 5) − 0.30 (H − 8 → L + 1)	
4.88	254.0	0.0122	0.60 (H − 10 → L) − 0.19 (H → L + 5)	
4.92	252.1	0.0357	0.56 (H − 4 → L + 3) − 0.22 (H − 6 → L + 3)	
4.95	250.4	0.0114	0.57 (H − 6 → L + 3) − 0.24 (H − 5 → L + 3)	
5.02	247.2	0.1146	0.48 (H − 8 → L + 3) − 0.24 (H → L + 4)	
5.06	244.8	0.0278	0.59 (H − 9 → L + 1) + 0.17 (H − 8 → L + 1)	
5.09	243.5	0.1483	0.50 (H − 5 → L + 3) + 0.18 (H − 12 → L)	240 (sh)
5.11	242.8	0.0020	0.51 (H − 2 → L + 4) + 0.28 (H − 1 → L + 4)	
5.12	242.4	0.0135	0.54 (H → L + 4) + 0.29 (H → L + 5)	
5.14	241.3	0.0244	0.35 (H − 1 → L + 5) + 0.27 (H → L + 4)	
5.20	238.6	0.0281	0.44 (H − 12 → L) − 0.28 (H − 1 → L + 5)	
5.23	237.3	0.0067	0.38 (H − 11 → L + 2) + 0.29 (H − 11 → L + 1)	
5.25	236.1	0.0098	0.49 (H − 14 → L) − 0.23 (H − 3 → L + 4)	
5.26	235.6	0.1197	0.52 (H − 9 → L + 2) + 0.28 (H − 8 → L + 2)	
5.30	233.9	0.0044	0.55 (H − 8 → L + 2) − 0.29 (H − 9 → L + 2)	
5.41	229.3	0.0024	0.65 (H − 7 → L + 3) − 0.12 (H − 12 → L + 1)	
5.43	228.2	0.0005	0.56 (H − 10 → L + 2) − 0.30 (H − 10 → L + 1)	
				210 (31 200)

[a] Principal electronic configurations; H and L stand for HOMO and LUMO, respectively. [b] In methanol solution, reference 1.

Another noteworthy aspect of the IR spectrum concerns the carbonyl vibrations of the YM framework. These are responsible for the strong, broad band with maximum at 1633 cm^{-1}, flanked by prominent features at 1643 and 1623 cm^{-1}. According to the PED in Table 3, of the four carbonyl stretching coordinates of YM, those associated with the C_9═O, $C_{8'}$═O, and C_{13}═O bonds give rise to vibrational modes having a specific, dominant character and high frequency. Instead, as a direct consequence of the $(C_7)O-H\cdots O(C_{12})$ H-bond, the C_{12}═O stretching coordinate, related to the "left-hand" amidic linkage, has a reduced strength (the calculated force constant is 9.47 versus 11.24 md $Å^{-1}$ for C_9═O, 10.89 md $Å^{-1}$ for $C_{8'}$═O, and 10.69 md $Å^{-1}$ for C_{13}═O) and is extensively coupled with other internal coordinates. It is predicted to contribute only to modes falling under 1600 cm^{-1}.

3.2.3. NMR Chemical Shifts. The results of the CSGT-DFT calculations for the ^{13}C NMR chemical shifts together with the experimental values[1] are reported in Table 4. Again, the differences between the DFT predictions for the two most preferred conformational isomers YM1 and YM2 are of minor importance. In both cases, a comprehensive reproduction of the experimental chemical shifts has been obtained. However, it must be stressed that, as a consequence of the "structure revision" mentioned in the introduction, the previous assignments[1] of the experimental signals of the pairs $C_{4''}/C_{7''}$ and $C_{5''}/C_{6''}$ have been interchanged in Table 4.

The most characteristic ^{13}C chemical shifts of YM are those of carbonyl carbon atoms, which are deshielded in a different degree. In particular, the thioester carbonyl resonates at 22 ppm lower field than the amide carbonyls. Therefore, it is very satisfying to remark that the large variation of δ(CO) along the sequence C_{12}, C_{13} (161.9) → $C_{8'}$(178.5) → C_9 (183.4) is accounted for fairly well by the theoretical results (Table 4). Another noteworthy point is that the DFT estimate (δ 9.4) of the methyl chemical shift of the thiomethyl ester is in good agreement with experiment (δ 11.1), in line with the previous

TABLE 3: Observed and Calculated Frequencies (cm^{-1}) and Assignment with Potential Energy Distribution in %

	YM1		YM2	
obs[a]	calcd	PED and assignment[b]	calcd	PED and assignment[b]
	2927	93 C_5H stretch	2944	99 C_5H stretch
	2924	99 C_5H stretch	2928	93 C_5H stretch
2925	2915	99 $C_{11}H$ stretch	2915	98 $C_{11}H$ stretch
	2912	90 C_4H stretch	2913	89 C_4H stretch
	2912	99 $C_{14}H$ stretch	2910	99 $C_{14}H$ stretch
2852	2826	99 O_7H stretch	2832	99 O_7H stretch
1643	1660	80 C_9O stretch	1661	80 C_9O stretch
1633	1646	78 C_8O stretch	1647	76 C_8O stretch
	1641	46 CC stretch	1640	44 CC stretch
1623	1635	55 $C_{13}O$ stretch	1631	33 CC stretch
	1631	36 CC stretch	1624	47 $C_{13}O$ stretch
	1592	21 $C_{12}O$ stretch	1598	49 CC stretch
	1588	43 CC stretch	1592	20 $C_{12}O$ stretch

[a] Solid, ref 4. [b] Potential energy distribution in %.

TABLE 4: Experimental and Calculated ^{13}C NMR Chemical Shifts Relative to TMS

position	expt[a]	YM1	YM2	position	expt	YM1	YM2
2	133.4	131.2	131.3	4′a	24.0	23.2	24.0
3	107.8	105.3	105.3	5′	55.6	53.3	53.9
3a	118.6	117.0	117.0	6a	161.9	161.9	163.0
3b	122.0	119.4	119.6	7′	112.8	114.9	110.1
4	28.2	27.1	27.1	8′	178.5	175.3	173.9
5	53.8	52.1	52.2	8′a	132.7	131.3	130.0
6a	128.9	130.6	130.6	12	161.9	159.5	159.4
7	140.5	145.7	145.7	2″	129.2	127.3	126.3
8	134.5	135.0	135.1	3″	107.6	104.6	107.5
8a	136.0	131.7	131.8	4″	104.6	104.2	104.8
9	183.4	183.3	183.3	5″	144.8	144.6	146.7
10	11.1	9.4	9.5	6″	150.4	149.8	150.1
11	60.4	56.6	56.5	7″	94.5	89.0	88.8
2′	130.4	125.7	126.0	7″a	133.1	130.2	130.8
3′	107.6	104.4	104.6	13	161.9	160.2	161.6
3′a	130.5	126.6	127.6	14	55.9	52.0	51.9
3′b	31.5	31.7	32.8				
4′	26.1	24.6	24.9				

[a] In pyridine solution, reference 1.

reformulation of this subunit of YM from thioacetate to thiomethyl ester.[3] Indeed, a typical resonance of aryl thioacetates occurs at δ 30.[25] Finally, it must be remarked that the DFT predictions correctly match the significant downfield sequence shown by the indole protons $C_{7''}$−H, C_3−H, and $C_{4''}$−H: expt. 7.24, 7.52, and 7.64 for YM,[1,3] versus calcd 6.40, 6.59, and 6.89 for YM1.

Because the spectroscopic properties reflect a complex balance of stereoelectronic factors in the YM framework, the good correspondence between calculated and experimental values for both IR and NMR data leads further support to the theoretically predicted conformational preferences.

3.3. Protonation Effects. As shown in Figure 1, the YM molecule bears eight oxygen atoms, five nitrogen atoms, and one sulfur atom each of which represents a potential site of protonation. Among them, however, the second and fourth nitrogen atoms are part of the rotatable bonds corresponding to torsion angles τ_1 and τ_3, respectively. It is therefore intriguing to investigate how protonation of these backbone atoms could affect the geometry of YM. Because each one of these N-sp^2 atoms can be approached by H^+ either from above or below the mean molecular plane of YM, four protonated forms of the YM1 conformer can be conceived. The optimized geometries of three N_6-protonated forms of YM1 are shown in Figure 6. As can be seen from this figure, in each case protonation has a dramatic effect on the equilibrium conformation of YM1 (Figure 2) as a result of pyramidalization of the protonated nitrogen atom.

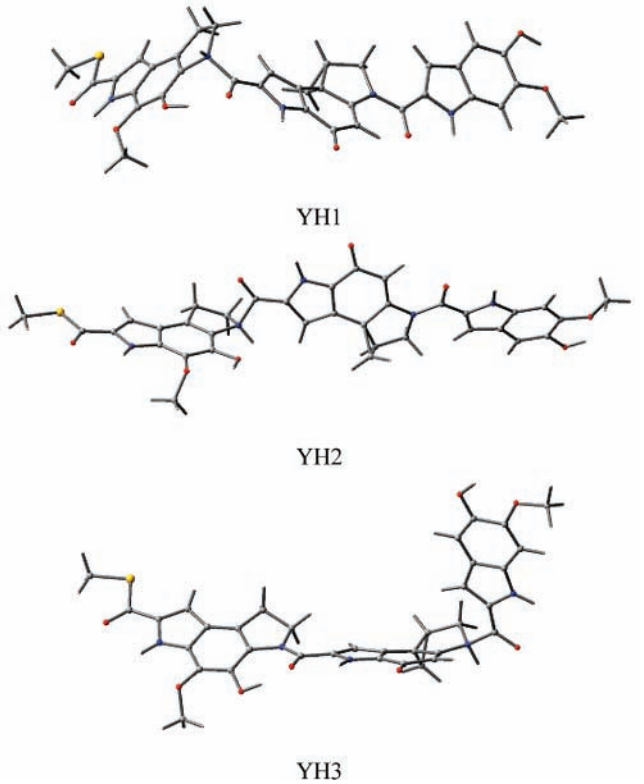

Figure 6. DFT-optimized geometries of three protonated forms of YM1: YH1 (top), YH2 (center), and YH3 (bottom).

Protonation of N_6 from the upper side of YM1 mean plane results in a V-shaped protonated form (YH1) characterized by the (nonbond) angle $C_2N_6C_{7'}$ of 108°. Protonation does not disrupt the intramolecular H-bond in the $(C_7)O-H\cdots O(C_{12})$ unit of YM1 although the optimized structural parameters of YH1 [O−H 0.989 Å, H···O 1.838 Å, O···O 2.785 Å, and angle O−H···O 159.5°] indicate that the H-bond is somewhat weakened with respect to the unprotonated conformer.

Protonation of N_6 from the bottom side of YM1 mean molecular plane generates a different protonated species YH2, where the left-side unit is nearly normal to the central unit (Figure 6). Here, the intramolecular H-bond in the $(C_7)O-H\cdots O(C_{12})$ unit is completely destroyed by protonation (O···O 3.876 Å). When $N_{6'}$ is protonated from the upper side of the mean molecular plane of YM1, the geometry of this protonated form cannot be optimized because of the steric clash between the right side unit and the cyclopropane moiety belonging to the central unit. On the other hand, protonation of $N_{6'}$ from the lower side of YM1 yields the protonated species YH3 (Figure 6), where the right-side unit of YM is almost perpendicular to the central unit. Interestingly, the intramolecular H-bond in YH3 is not weakened by protonation [O−H 1.009 Å, H···O 1.584 Å, O···O 2.567 Å, and angle O−H···O 163.5°].

We also computed the proton affinity (PA) of YM with respect to the corresponding conjugated acid species YH1−YH3 according to the standard formulas employed in the literature.[26] The PA values are collected in Table 5, together with the ZPE-corrected energy differences computed in vacuo at the BLYP/6-31G(d, p) level of theory (the corresponding values obtained from single-point PCM−DFT calculations are given in parenthesis). As can be seen from Table 5, protonation of N_6 gives the conjugated acid YH2 which is the most favored

TABLE 5: Torsion Angles (Deg) and Relative Energies (kcal mol^{-1}) of Protonated Forms of YM1 and Proton Affinity (kcal mol^{-1}) of the Conjugated Bases; in Parentheses, Single-Point PCM Results for Water Solution

conformer	τ_1	τ_2	τ_3	τ_4	μ	ΔE^a	PA^a
YH1	−86.6	176.7	8.9	−171.5	6.2 (10.6)	6.18 (5.99)	217.0 (259.3)
YH2	−39.8	−178.9	8.8	−172.1	9.5 (12.3)	0 (0)	223.2 (264.9)
YH3	−2.7	166.4	121.2	135.0	27.0 (33.9)	7.15 (3.23)	216.0 (261.1)

[a] Inclusive of zero-point energy contribution.

among the protonated adducts of YM1 (PA = 223.15 kcal mol^{-1}). The reason for this preference is due to the higher stability of the corresponding adduct YH2 in comparison to both YH1 and YH3, as shown by the relative ZPE-corrected energy values reported in Table 5. These results indicate that protonation of the backbone N-sp^2 atoms is likely to disrupt the pharmacological activity of YM which must adopt a nearly planar conformation in order to bind and alkylate DNA in the minor groove.[1−5]

3.4. Oxidized Adducts. It is well documented that the thiomethyl groups (∼S−Me) of methionine residues (Met) in proteins can readily be oxidized to the corresponding methionine sulfone (∼SO−Me) and methionine sulfoxide (∼SO$_2$−Me) forms by a variety of inorganic oxidants.[27] An important example of this kind is represented by the oxidation of Met35 residue in the amyloid β-peptide which, being toxic to neurons, is linked to the insurgence of Alzheimer's disease.[28] Because YM contains a thiomethyl ester subunit (Figure 1), its oxidation in vivo could result in the loss of pharmacological activity. Hence, we investigated two mono- and one di-oxidized forms of YM (YO1−YO3), whose optimized structures are displayed in Figure 7. According to the DFT results, oxidation of YM thiomethyl group does not significantly affect the conformation of the most stable conformer YM1, as shown by the torsion angles reported in Table 6. Interestingly, the dipole moment computed for all three oxidized forms is slightly lower than that computed in the gas-phase for YM1 (10.20 Debye). Furthermore, the semi-oxidized forms possess nearly the same

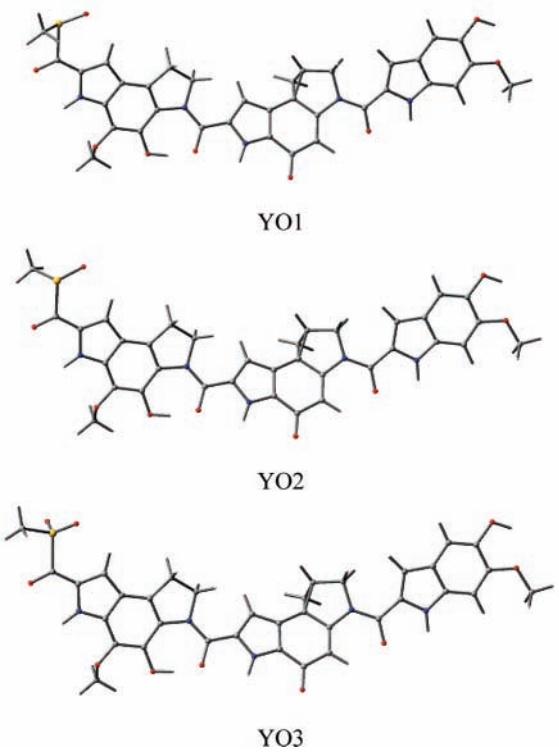

Figure 7. DFT-optimized geometries of three oxidized adducts of YM1: YO1 (top), YO2 (center), and YO3 (bottom).

TABLE 6: Torsion Angles (Deg), Dipole Moment (Debye), and Relative Energies (kcal mol^{-1}) of Oxidized Forms of YM1; in Parentheses, Single-Point PCM Results for Water Solution

conformer	τ_1	τ_2	τ_3	τ_4	μ	ΔE^a
YO1	−2.7	166.3	7.8	−170.5	9.1 (11.5)	0 (0)
YO2	−2.4	166.2	8.1	−170.8	9.8 (12.5)	0.05 (0.12)
YO3	−2.5	166.4	8.0	−170.6	9.4 (11.3)	

[a] Inclusive of zero-point energy contribution.

stability, YO1 being only 0.05 kcal mol^{-1} (ZPE-corrected value) more stable than YO2. This energy difference increases to 0.12 kcal mol^{-1} in a continuum water environment as suggested by PCM−DFT results.

3.5. YM−adenine Adduct. The formation of this adduct has provided important clues on the DNA alkylation properties of YM, which are responsible for its remarkable anticancer activity.[1−5] Indeed, as established experimentally by Tichenor et al.,[5] it shares the sites of nucleophilic attack (adenine N$_3$) and binding of the alkylation product (addition to the least substituted cyclopropane carbon C$_{4'}$ of YM). Here, the molecular structure of the adduct was explored at the same DFT level, BLYP/6-31G(d, p), employed for the free YM molecule. The binding model of the adduct was built by formal assemblage of conformer YM1 and adenine while taking into account the stereochemistry of the carbon C$_{4'a}$ as suggested by Tichenor et al.[5] As shown in Figure 8, the conformation of the adduct is mainly governed by two torsion angles, φ_1(C$_{3'b}$−C$_{4'a}$−C$_{4'}$−N$_{3'''}$) and φ_2(C$_{4'a}$−C$_{4'}$−N$_{3'''}$−C$_{2'''}$). Owing to a manifold of possible structures for the YM−adenine adduct, semiempirical AM1 calculations were carried out by independently varying torsion angles φ_1 and φ_2 in the 0−360° range. Thus, four stable adduct conformers were identified and subsequently optimized with DFT.

Table 7 reports the relative energies and torsion angles of the four adduct conformers A1−A4, while Figure 9 depicts the structures of the two most stable ones as computed in the gas phase (A1: $\varphi_1 = 162.1°$, $\varphi_2 = 104.5°$; A2: $\varphi_1 = 164.9°$, $\varphi_2 = -94.8°$). Interestingly, single-point energy PCM-DFT calculations indicate that the A3 conformer becomes slightly more stable than A2 ($\Delta E \sim 0.3$ kcal mol^{-1}) when surrounded by a continuum water environment. We remark, however, that both

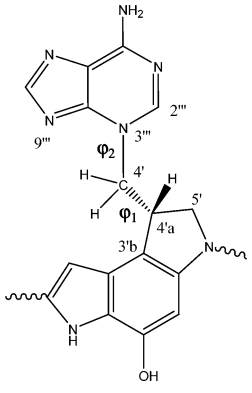

Figure 8. Formula and atom numbering of the YM−adenine adduct.

TABLE 7: Torsion Angles (Deg), Dipole Moment (Debye), and Relative Energies (kcal mol^{-1}) of the Adduct Conformers of YM1; in Parentheses, Single-Point PCM Results for Water Solution

conformer	φ_1	φ_2	μ	ΔE^a
A1	162.1	104.5	9.9 (12.5)	0 (0)
A2	164.9	−94.8	3.0 (3.2)	2.44 (1.76)
A3	−58.3	88.7	3.7 (3.7)	2.94 (1.44)
A4	65.9	67.9	7.7 (10.0)	5.26 (2.44)

[a] Inclusive of zero-point energy contribution.

A3 and A4 are characterized by folded-like structures, with their adenine moieties being almost π-stacked relative to the central aromatic moiety of YM. Although both of these conformers are likely to exist in solution, they certainly cannot be attained when YM alkylates adenine in the minor groove of DNA.

It is also interesting to note the peculiar arrangement of the adenine unit in A1 and A2 that lies under the average plane of the molecular framework of YM. In A1, the diazole ring of adenine points toward the left-hand unit of YM and the distance between $N_{9'''}$ and the H atom attached to $C_{3'}$ is only 2.766 Å. On the other hand, in A2 (ΔE = 2.44 kcal mol^{-1}) the adenine moiety is rotated in the opposite direction and the shortest noncontact distance (3.075 Å) is that between the H atoms connected to $C_{2'''}$ and $C_{3'}$.

According to experimental characterization of the isolated adduct,[5] the unambiguous assignment of its structure relies upon the observation of some NMR key signals, most importantly those associated with the carbons within or proximal to the methylenic bridge, i.e., $C_{2'''}$, $C_{4'}$, $C_{4'a}$, and $C_{5'}$. For these diagnostic resonances, it is very gratifying to remark the good correspondence between CSGT-DFT estimates for A1 and experimental values (in DMF):[5] $C_{2'''}$ (calc. 139.1, expt. 144.6), $C_{4'a}$ (41.8, 41.1), $C_{5'}$ (53.6, 54.8), and $C_{4'}$ (53.9, 54.3), with the $C_{4'a}$ methine peak falling upfield of the adjacent $C_{4'}$ and $C_{5'}$ methylene peaks. Furthermore, there is a substantial accord also for two most symptomatic protons, the cyclopropane $C_{4'a}$−H (calc. 4.23, expt. 4.52) and the adenine $C_{2'''}$−H (calc. 7.56, expt. 8.28). On this basis, the present structural model of the YM−adduct may be regarded as consistently reliable.

Finally, we would like to comment about the DNA-alkylation reaction as triggered by yatakemycin. So far, two hypothesis have been formulated for DNA-alkylating agents. The first one is concerned with the acid catalysis mediated by the sugar−phosphate backbone of DNA, as proposed by Hurley and Warpehoski.[29,30] Accordingly, the carbonyl group on the aromatic moiety bearing the cyclopropane group would be protonated by a neighboring phosphate group thereby triggering the alkylation reaction on adenine. Recent computational studies, however, ruled out such possibility while establishing that the catalytic effect arising from cation (e.g., Na^+ or NH_4^+) complexation is more important.[31] The second hypothesis has been put forward by Boger and co-workers on the basis of experiments complemented by docking calculations and classical molecular dynamics (MD) simulations.[32,33] According to these authors, binding of the flat-like duocarmycin SA molecule to the minor groove of DNA induces a conformational change which decreases the π-electron delocalization throughout the ligand thus activating the reactive methylene group. Given that duocarmycin SA and yatakemycin have an identical central unit and a similar right-hand unit, a like mechanism can be postulated for the latter as well. Our DFT results, however, indicate an opposite scenario. Figure 10 compares the gas-phase optimized structures of YM1 and A2 (i.e., the "bioactive" conformer, see ref 5) as viewed along the molecular plane of the central unit.

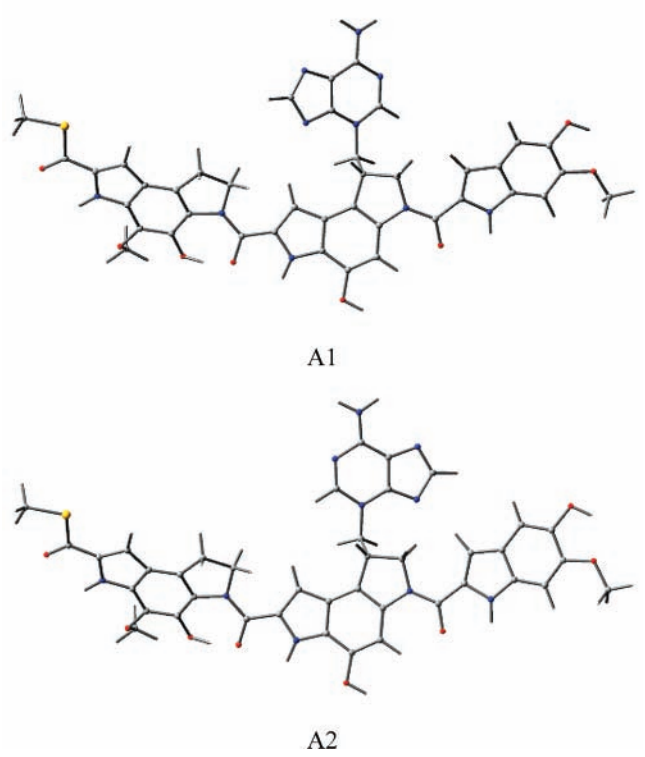

Figure 9. DFT-optimized geometries of the YM−adenine adduct conformers A1 (top) and A2 (bottom).

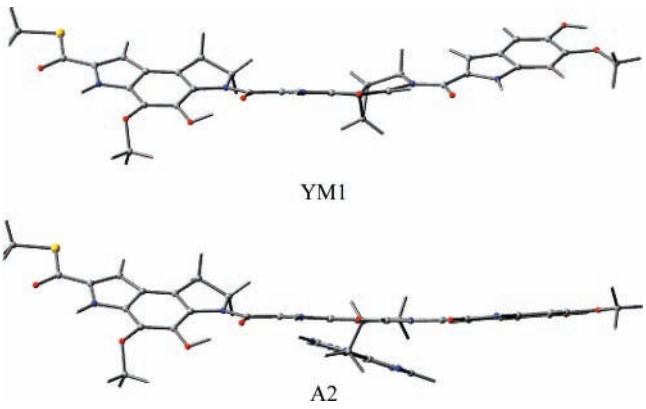

Figure 10. DFT-optimized geometries of YM1 (top) and A2 (bottom) as viewed along the molecular plane containing the central pyrroloindole unit.

As seen in this figure, covalent binding of adenine to YM1 flattens the central and right-hand units of the A2 adduct whereas this is not the case in the isolated YM1 molecule where, a part from the bridging methylene group, three atoms of the central unit and all those of the right-hand unit appear being significantly out-of-plane. Hence, as far as electronic effects are concerned, alkylation increases the π-electron conjugation throughout the YM molecule. Of course, steric and polarization effects induced by the DNA scaffold, both of which are not considered here, may alter the conformation of the covalently bonded YM molecule. Recent molecular simulation studies with the Car−Parrinello MD method, however, do not support such possibility while indicating that the duocarmycin SA molecule is less flexible when it is covalently bonded to DNA that in the free state.[34]

At this point, given the above results and observations, we formulate the following hypothesis for the DNA-alkylation reaction triggered by yatakemycin. When YM interacts with the minor groove of DNA, the alkylation reaction takes place

so as to release the steric strain accumulated in the central part of the ligand. To support this "steric strain release" hypothesis, we have computed the free energy (ΔG^{298}) of the reaction YM1 + Adenine → A1 at the BLYP/6-31G(d, p) level of theory. The computed value of ΔG^{298} (gas-phase) corresponds to −1.16 kcal mol^{-1}, thus suggesting that the adenine alkylation reaction triggered by yatakemycin is exergonic. The value of ΔG^{298} (gas-phase) corresponding to the formation of A2 from YM1 and adenine is only 0.94 kcal mol^{-1}. These results appear being in qualitative agreement with the experimental observation made by Parrish et al.[2] that the DNA alkylation reaction carried out at 100 °C is not reversible.

4. Concluding Remarks

The structure and conformational preferences of YM, a new and most potent antitumor antibiotic, have been studied with DFT calculations, performed at the BLYP/6-31G(d, p) level. Among the 12 stable conformers investigated, two (referred to as YM1 and YM2) are predicted to have similar energies while being distinctly more stable than the others in the gas-phase. In polar solvents, such as water, the lowest energy conformer is also found to predominate. These results suggest that YM should exist as a mixture of the two most preferred conformers YM1 and YM2 in polar mediums.

The structure of YM has also been investigated through its UV−visible, IR, and NMR spectroscopic properties. On the whole, the correspondence between experimental data and calculated values, obtained for the two favored conformers, is very satisfactory. In particular, the low-lying electronic excited states have been characterized in terms of the main one-electron jumps. On the other hand, the strong IR band at 2852 cm^{-1} may be recognized as a peculiar fingerprint of YM. Indeed, it is due to the O−H stretching of the $(C_7)O-H\cdots O(C_{12})$ fragment, held together by a strong intramolecular H-bond. Furthermore, the pattern of NMR chemical shifts of carbonyl carbon atoms and indole protons, which are the more sensitive to local stereoelectronic factors, is accounted for fairly well. Therefore, the consistent reproduction of the spectroscopic data gives good support to the present structural characterization of YM.

The effects of both protonation of the backbone nitrogen atoms and oxidation of the thiomethyl group on the geometry of the most stable conformer of YM were also analyzed. Our results indicate that protonation strongly affects the structure of YM1 with consequent loss of planarity which might affect the pharmacological activity of the natural product. In contrast, oxidation does not change the structure of the most stable conformer while only slightly decreases its dipole moment.

Finally, because the biological activity of YM originates from the central cyclopropane subunit, the structural arrangement of the representative YM−adenine adduct has been theoretically modeled and found consistent with the experimental spectroscopic evidence. From these results it appears that DNA alkylation by YM increases the π-electron delocalization throughout the ligand. Hence, we formulated the hypothesis that the alkylation reaction takes place so as to release the steric strain accumulated in the central unit of YM where the cyclopropane subunit is located.

Acknowledgment. The authors thank Prof. Tohru Fukuyama (The University of Tokyo) for providing a copy of the IR spectrum and Prof. Yasuhiro Igarashi (Toyama Prefectural University) for supplying a reprint of reference 1 and a copy of the UV−visible spectrum. F.P. thanks the financial support of the 21st century COE project "Unexplored Chemistry-Giant Molecules and Complex Systems" of Tohoku University. The authors thank the reviewers for helpful comments.

Supporting Information Available: Total energies and atomic coordinates of the preferred conformers of yatakemycin and its adduct with adenine. This material is available free of charge via the Internet at http://pubs.acs.org.

References and Notes

(1) Igarashi, Y.; Futamata, K.; Fujita, T.; Sekine, A.; Senda, H.; Naoki, H.; Furumai, T. *J. Antibiot.* **2003**, *56*, 107.

(2) Parrish, J. P.; Kastrinsky, D. B.; Wolkenberg, S. E.; Igarashi, Y.; Boger, D. L. *J. Am. Chem. Soc.* **2003**, *125*, 10971.

(3) Tichenor, M. S.; Kastrinsky, D. B.; Boger, D. L. *J. Am. Chem. Soc.* **2004**, *126*, 8396.

(4) Okano, K.; Tokuyama, H.; Fukuyama, T. *J. Am. Chem. Soc.* **2006**, *128*, 7136.

(5) Tichenor, M. S.; Trzupek, J. D.; Kastrinsky, D. B.; Shiga, F.; Hwang, I.; Boger, D. L. *J. Am. Chem. Soc.* **2006**, *128*, 15683.

(6) Frisch, M. J.; Trucks, G. W.; Schlegel, H. B.; Scuseria, G. E.; Robb, M. A.; Cheeseman, J. R.; Montgomery, J. A., Jr.; Vreven, T.; Kudin, K. N.; Burant, J. C.; Millam, J. M.; Iyengar, S. S.; Tomasi, J.; Barone, V.; Mennucci, B.; Cossi, M.; Scalmani, G.; Rega, N.; Petersson, G. A.; Nakatsuji, H.; Hada, M.; Ehara, M.; Toyota, K.; Fukuda, R.; Hasegawa, J.; Ishida, M.; Nakajima, T.; Honda, Y.; Kitao, O.; Nakai, H.; Klene, M.; Li, X.; Knox, J. E.; Hratchian, H. P.; Cross, J. B.; Bakken, V.; Adamo, C.; Jaramillo, J.; Gomperts, R.; Stratmann, R. E.; Yazyev, O.; Austin, A. J.; Cammi, R.; Pomelli, C.; Ochterski, J. W.; Ayala, P. Y.; Morokuma, K.; Voth, G. A.; Salvador, P.; Dannenberg, J. J.; Zakrzewski, V. G.; Dapprich, S.; Daniels, A. D.; Strain, M. C.; Farkas, O.; Malick, D. K.; Rabuck, A. D.; Raghavachari, K.; Foresman, J. B.; Ortiz, J. V.; Cui, Q.; Baboul, A. G.; Clifford, S.; Cioslowski, J.; Stefanov, B. B.; Liu, G.; Liashenko, A.; Piskorz, P.; Komaroni, I.; Martin, R. L.; Fox, D. J.; Keith, T.; Al-Laham, M. A.; Peng, C. Y.; Nanayakkara, A.; Challacombe, M.; Gill, P. M. W.; Johnson, B.; Chen, W.; Wong, M. W.; Gonzalez, C.; Pople, J. A. *Gaussian 03*, revision D.01; Gaussian Inc.: Wallingford, CT, 2004.

(7) Becke, A. D. *Phys. Rev.* **1988**, *A38*, 3098.

(8) Lee, C.; Yang, W.; Parr, R. G. *Phys. Rev.* **1988**, *B41*, 785.

(9) Dunlap, B. I. *J. Mol. Struct. (THEOCHEM)* **2000**, *529*, 37.

(10) Wilson, E. B.; Decius, J. C.; Cross, P. C. *Molecular Vibrations*; McGraw-Hill: New York, 1945.

(11) Rauhut, G.; Pulay, P. *J. Phys. Chem.* **1995**, *99*, 3093.

(12) Pipek, J.; Mezey, P. G. *J. Chem. Phys.* **1989**, *90*, 4916.

(13) Sannigrahi, A. B.; Kar, T. *Chem. Phys. Lett.* **1990**, *173*, 569.

(14) Cheeseman, J. R.; Frisch, M. J.; Devlin, F. J.; Stephens, P. J. *J. Phys. Chem. A.* **2000**, *104*, 1039.

(15) Becke, A. D. *J. Chem. Phys.* **1993**, *98*, 5648.

(16) Woon, D. E.; Dunning, T. H., Jr. *J. Chem. Phys.* **1993**, *98*, 2823.

(17) Stratmann, R. E.; Scuseria, G. E.; Frisch, M. J. *J. Chem. Phys.* **1998**, *109*, 8218.

(18) Keith, T. A.; Bader, R. F. W. *Chem. Phys. Lett.* **1993**, *210*, 223.

(19) Rychnovsky, R. D. *Org. Lett.* **2006**, *8*, 2895.

(20) Barone, V.; Cossi, M.; Tomasi, J. *J. Chem. Phys.* **1997**, *107*, 3210.

(21) Böes, E. S.; Livotto, P. R.; Stassen, H. *Chem. Phys.* **2006**, *331*, 142.

(22) Parrish, J. P.; Trzupek, J. D.; Hughes, T. V.; Hwang, I.; Boger, D. L. *Bioorg. Med. Chem.* **2004**, *12*, 5485.

(23) Kwasniewski, S. P.; Deleuze, M. S.; François, J. P. *Int. J. Quantum Chem.* **2000**, *80*, 672.

(24) Hsu, C.-P.; Hirata, S.; Head-Gordon, M. *J. Phys. Chem. A* **2001**, *105*, 451.

(25) Jordan, F.; Kudzin, Z.; Witczak, Z.; Hoops, P. *J. Org. Chem.* **1986**, *51*, 571.

(26) The proton affinity (PA) of a general base (B) with respect to its conjugated acid (BH^+) is computed using the equation: PA(B) = Δ, E − Δ, ZPE, where Δ, $E = E(B) - E(BH^+)$ and Δ, ZPE = ZPE(B) − ZPE-(BH^+). See, for example: Maksić, Z. B.; Kovačević, B. *J. Phys. Chem. A* **1998**, *102*, 7324.

(27) Vogt, W. *Free Rad. Biol. Med.* **1995**, *18*, 93.

(28) Schöneich, C. *Arch. Biochem. Biophys.* **2002**, *397*, 370.

(29) Hurley, L. H.; Warpehoski, M. A. *Chem. Res. Toxicol.* **1988**, *1*, 315.

(30) Warpehoski, M. A.; Harper, D. E. *J. Am. Chem. Soc.* **1995**, *117*, 2951.

(31) Freccero, M.; Gandolfi, R. *J. Org. Chem.* **2005**, *70*, 7098.

(32) Boger, D. L.; Johnson, D. S. *Angew. Chem., Int. Ed.* **1996**, *35*, 1438.

(33) Schnell, J. R.; Ketchem, R. R.; Boger, D. L.; Chazin, W. J. *J. Am. Chem. Soc.* **1999**, *121*, 5645.

(34) Spiegel, K.; Rothlisberger, U.; Carloni, P. *J. Phys. Chem. B* **2006**, *110*, 3647.